Monte Carlo Study of Polymer Chains in Dilute and Nondilute Solution with Varying Solvent Conditions

Antonio López Rodriguez and Juan J. Freire*

Departamento de Quimica Fisica, Facultad de Ciencias Quimicas, Universidad Complutense, 28040 Madrid, Spain

Received September 20, 1990; Revised Manuscript Received January 18, 1991

ABSTRACT: Monte Carlo calculations of dilute and more concentrated polymer solution systems in a simple cubic lattice have been performed for different values of the polymer length and solvent (or temperature) conditions. The following properties have been obtained: dimensions, single-chain scattering form factors, diffusion coefficients in dilute solution with hydrodynamic interactions (via the Kirkwood formula), and end-to-end distribution functions. These results are analyzed in light of theoretical predictions and experimental data.

Introduction

The method of Monte Carlo simulations in lattices constitutes a very popular and powerful numerical procedure to investigate the behavior of polymer chains.[1] The use of lattice coordinates leads to drastic reductions in computational time while, for many interesting properties, the lattice restrictions do not introduce significant distortions with respect to more realistic models (moreover, the recent introduction of fluctuating bond techniques[2] may serve to eliminate a good deal of these restrictions, whenever it is necessary). The method is especially adequate for long flexible chains, since most of their properties are governed by model-independent scaling laws.[3] Then, it can be applied to study equilibrium properties of polymeric systems. The dynamics of polymer chains can be also investigated if a conveniently chosen simulation step is made equivalent to an arbitrary time unit, though some technical complications due to the presence of intramolecular hydrodynamic interactions in dilute systems[4] cannot be rigorously addressed through Monte Carlo samplings.

Consequently, several types of Monte Carlo algorithms have been extensively explored in the past years by different groups. The algorithms differ basically in the definition of conformational changes that can be carried out in a simulation step. The choice of a particular algorithm is determined by the system and properties to be investigated. Thus, the analysis of global equilibrium properties of single chains is performed very efficiently by the Pivot algorithm,[5] which involves global changes in a part of the chain in each simulation cycle. However, for nondilute systems, the adequate algorithms should be restricted to more localized changes.

We have built an algorithm to study equilibrium properties on nondilute systems in a simple cubic lattice. This algorithm combines global, though moderate, changes represented by reptations, which are customarily employed for these systems,[1] since they allow for a fast relaxation, with local motions as the bents and crankshafts and terminal motions, employed in dynamical studies.[6,7] The localized motions permit a diverse number of ways to change the internal structure of the chains, which may be useful for properties directly depending on this structure (as the quadratic mean radius of gyration, $\langle S^2 \rangle$). Furthermore, as the proportion between localized inner motions and reptation is governed by a parameter introduced in the simulation (as will be detailed in next section) the algorithm can be conveniently applied to dynamic properties (for which reptations are no longer applicable) without an extensive modification of the program codes. The method is mainly inspired in the procedures employed by Kolinski et al.[8] for single chains in tetrahedrical lattices and also in their general method for thermal equilibration previous to dynamic simulations.[9]

As a difference with respect to most studies on nondilute systems, we generate self-avoiding conformations with an attractive potential $-\epsilon$ (expressed through the parameter ϵ/k_BT, where k_BT is the Boltzmann factor) for nonbonded polymer units placed in adjacent lattice sites. This allows us to investigate different temperature or solvent conditions. In this article, we report results for (a) mean dimensions, expressed as the mean quadratic end-to-end distance, $\langle R^2 \rangle$, and also as $\langle S^2 \rangle$ for different values of the polymer number of units, N, the polymer volume fraction, Φ, and also of ϵ/k_BT; (b) the form factor of single chains, $S(q)$, depending on the different parameters and also on the scattering variable q; (c) the sum of reciprocal distances between different internal units in a chain, $S_r = \sum_i^N \sum_j^N \langle R_{ij}^{-1} \rangle$, which for a dilute chain, is directly related to hydrodynamic properties according to approximate hydrodynamic treatments[4] (this way, we have obtained the dilute limit of the translational diffusion coefficient, D_0); and (d) finally, the end-to-end distance distribution function, $F(R)$, and comparison of the results to theoretical predictions that correspond to the different concentrations and solvent conditions.[3]

Methods

We have built n self-avoiding polymer chains, each with N bonded units in the sites of a simple cubic lattice. The sites are labeled with an index that indicates whether or not they are occupied. If the site is empty, we assume it contains a given number of solvent molecules with the volume of a polymer unit. The attractive potential is added for each pair of nonbonded units (belonging or not to the same chain) placed on neighboring lattice sites, whose distance, b, acts as the unit length in the calculations. Periodic boundary conditions are established according to standard methods. The lattice size is described by a cube length L, which is fixed long enough following the criterion

$$L \geq 2N^{1/2} + 5 \quad (1)$$

This criterion is in accordance with previously established procedures.[10]

Following previous methods,[8] we assign different probabilities to end and inner motions so that their ratio is $2/(x_pN)$, where x_p is an appropriately chosen parameter. After checking our initial results for a single chain with different values of x_p, we have fixed $x_p = 1/N$ as the most efficient choice. The higher number of localized terminal motions helps to introduce new bond vectors

0024-9297/91/2224-3578$02.50/0

Table I
Results for $\langle R^2 \rangle$ Obtained with Different Chain Lengths, Solvent Conditions, and Polymer Concentrations

		$\langle R^2 \rangle$				
Φ	ϵ/k_BT	$N = 36$	$N = 48$	$N = 60$	$N = 84$	ν_R
single chain	0	75.7 ± 0.6	108 ± 1	140 ± 2	216 ± 4	0.60 ± 0.01
	0.1	69.0 ± 0.6	97.9 ± 0.9	127 ± 2	197 ± 5	0.60 ± 0.01
	0.2	62.3 ± 0.6	86.7 ± 1	111 ± 2	162 ± 4	0.55 ± 0.01
	0.275	56.7 ± 0.6	77 ± 1	98 ± 1	139 ± 4	0.52 ± 0.01
	0.3	54.1 ± 0.6	74 ± 1	96 ± 2	129 ± 3	0.52 ± 0.01
	0.32	52.2 ± 0.5	71 ± 1	87 ± 2	118 ± 3	0.48 ± 0.01
	0.34	49.8 ± 0.4	68.5 ± 0.8	82 ± 1	113 ± 3	0.48 ± 0.01
	0.4	46.1 ± 0.5	58.6 ± 0.9	73 ± 2	88 ± 2	0.39 ± 0.01
	0.5	36.0 ± 0.4	45.1 ± 0.7	51.1 ± 0.9	54 ± 1	0.26 ± 0.01
0.38	0	64.0 ± 0.4	89.3 ± 0.6	108.1 ± 0.8	162 ± 1	0.532 ± 0.005
	0.1	61.9 ± 0.4	84.6 ± 0.6	107.1 ± 0.9	155 ± 1	0.531 ± 0.005
	0.2	60.3 ± 0.4	81.3 ± 0.7	102.2 ± 0.9	152 ± 1	0.535 ± 0.005
	0.3	57.7 ± 0.4	77.7 ± 0.6	98.7 ± 0.9	144 ± 1	0.530 ± 0.005
0.75	0	58 ± 1	76.2 ± 0.9	100 ± 3	135 ± 4	0.49 ± 0.02
	0.1	55.8 ± 0.8	76.0 ± 0.9	99 ± 3	137 ± 3	0.52 ± 0.02
	0.2	56.5 ± 0.7	77.4 ± 0.9	101 ± 3	143 ± 4	0.54 ± 0.02
	0.3	56.6 ± 0.6	76 ± 1	106 ± 2	145 ± 2	0.55 ± 0.01

that are then propagated by the otherwise inefficient bent motions, facilitating in this way the chain relaxation. Once an inner unit has been selected for a change, we find out whether the bonds attached to it can be involved in a bent or a randomly chosen 90° crankshaft motion, according to the limitations set by the single occupation rule.[7] If none of these alternative motions are possible, we reject the new conformation and, according to the Metropolis criterion, the old conformation is counted again in the Monte Carlo sampling. When a terminal unit is selected, we randomly choose between a localized motion where the end bond suffers a 90° rotation and a reptation where the end bond is suppressed and a new bond with random orientation is added at the opposite end. Again, the new conformation is rejected if it does not satisfy the single occupancy requirement. A further check is performed before the final acceptance of a new conformation; we investigate the possible change in the total attractive energy due to nonneighboring units in adjacent sites. Following the Metropolis rule, we accept the conformation if this change, ΔE, is negative. Otherwise, we choose a random number ξ between 0 and 1 and reject the new conformation unless the condition

$$\exp(-\Delta E/k_BT) > \xi \tag{2}$$

is satisfied.

The initial configuration is obtained by two alternative procedures. The first one, proposed by Kolinski et al.,[9] consists of selecting n lattice sites from which the chains grow up simultaneously (by random addition of beads). Once a chain has reached 6 units, a random choice is made in the successive steps between the further growing and the elementary motions previously described. This process continues until all the chains have the required number of units, N. Then, a relatively short thermal equilibration (on the order of (2–5) × 10^5 elementary motions or cycles) is performed, before starting the calculation of properties.

In particular cases with high values of N and Φ we have not been able to obtain fully grown chains with this procedure. (The reversal reptations proposed by Kolinski et al.[9] have not be attempted.) However, we have found useful a simpler method in which a whole chain is generated at once from each one of the n initial sites (maintaining the single occupation rule). This way, the chains grow remarkably fast, even for concentrated systems, but, then, a considerable longer thermal equilibration (of about 10^7 steps) is needed.

The results for different properties are calculated and recorded only for a reduced fraction of the generated cycles, since, except in the case of $\langle R^2 \rangle$, their calculation is as involving as the conformational changes, and, moreover, results corresponding to subsequent cycles are strongly correlated, being statistically redundant. Typically, the results extend for 10^7 cycles (after thermal equilibration), and they are recorded every 10^4 or 2 × 10^4 cycles. (For single chains we use 5 × 10^6 cycles, recorded every 10^2 cycles.) Even though, we have detected some correlations in certain cases. Then, the uncertainty associated with a given mean $\langle x \rangle$, obtained from n_s data, x_j, is calculated according to the method recently discussed by Bishop and Frinks[11]

$$\sigma_c = \sigma_d[1 + 2\sum_{j=1}^{n_c}(1 - j/n_s)\rho_j]^{1/2} \tag{3}$$

where σ_d is the uncertainty corresponding to noncorrelated data

$$\sigma_d^2 = [1/n_s(n_s - 1)]\sum_{j=1}^{n_s}[x_j - \langle x \rangle]^2 \tag{4}$$

and ρ_j is the correlation function evaluated as

$$\rho_j = [1/(n_s - j)]\sum_{k=1}^{n_s-j}[(x_k - \langle x \rangle)(x_{k+j} - \langle x \rangle)]/[\langle x^2 \rangle - \langle x \rangle^2] \tag{5}$$

As modifications in the formulas given in ref 11 (valid for a wide collection of data), we have introduced n_c as a cut-off corresponding to the term before a negative value for ρ_j is encountered (we assume that negative correlations are caused only by statistical noise in most samples) and have redefined ρ_j to be applicable even when $n_s - j$ is much smaller than n_s. Consequently, the formulas are now useful for samples constituted by a relatively small number of data.

Results and Discussion

(a) Dimensions. The values of $\langle R^2 \rangle$ and $\langle S^2 \rangle$ in a given cycle have been evaluated from the position of the units corresponding to the different chains. We have verified that, for dilute (single) chains of different lengths (up to 201 units) and $\epsilon/k_BT = 0$, our means and error bars are consistent with previously reported values.[4,5,7,12]

In Tables I and II we show results obtained for systematically chosen values of N, ϵ/k_BT, and Φ. We can observe that, for fixed values of the chain length and solving conditions, the results vary with changing concentration. In good solvent conditions, $\epsilon/k_BT \simeq 0$, the dimensions decrease with increasing polymer concentration as a consequence of the decrease of the polymer–solvent interactions that give rise to the excluded-volume effect. This is an effect well predicted by theory[3] and confirmed through neutron scattering of labeled polymers.[13] It has also been confirmed by several previous simulations of nondilute self-avoiding polymer systems,[12,14,15] so that the good solvent behavior of our present results for dimensions can only serve as a further verification for our algorithm. We have explicitly compared our variations with concentration with the results of ref 14, both sets of values being in excellent agreement. However, we can now observe how, though this trend persists for other small values of

Table II
Results for $\langle S^2 \rangle$

Φ	ϵ/k_BT	$\langle S^2 \rangle$ $N = 36$	$N = 48$	$N = 60$	$N = 84$	ν_S
single chain	0	12.01 ± 0.07	17.1 ± 0.1	22.2 ± 0.2	33.6 ± 0.6	0.593 ± 0.008
	0.1	11.13 ± 0.07	15.7 ± 0.1	20.4 ± 0.2	31.4 ± 0.6	0.590 ± 0.009
	0.2	10.20 ± 0.08	14.2 ± 0.1	18.2 ± 0.2	26.3 ± 0.4	0.551 ± 0.009
	0.275	9.46 ± 0.08	12.9 ± 0.1	16.6 ± 0.2	23.4 ± 0.5	0.53 ± 0.01
	0.3	9.14 ± 0.07	12.5 ± 0.1	16.0 ± 0.2	21.9 ± 0.4	0.52 ± 0.01
	0.32	8.88 ± 0.06	12.1 ± 0.1	14.9 ± 0.2	20.6 ± 0.4	0.50 ± 0.01
	0.34	8.63 ± 0.05	11.6 ± 0.1	14.2 ± 0.2	19.7 ± 0.4	0.48 ± 0.01
	0.4	8.08 ± 0.05	10.4 ± 0.1	13.0 ± 0.2	15.9 ± 0.3	0.41 ± 0.01
	0.5	6.76 ± 0.05	8.57 ± 0.09	9.8 ± 0.1	11.2 ± 0.2	0.323 ± 0.009
0.38	0	10.46 ± 0.05	14.57 ± 0.07	18.02 ± 0.09	26.6 ± 0.2	0.533 ± 0.005
	0.1	10.22 ± 0.04	13.95 ± 0.07	17.8 ± 0.1	25.8 ± 0.1	0.537 ± 0.003
	0.2	9.96 ± 0.04	13.47 ± 0.07	16.94 ± 0.09	25.0 ± 0.1	0.533 ± 0.003
	0.3	9.59 ± 0.04	12.97 ± 0.07	16.6 ± 0.1	23.7 ± 0.1	0.525 ± 0.004
0.75	0	9.5 ± 0.1	12.89 ± 0.06	16.7 ± 0.6	22.7 ± 0.5	0.51 ± 0.01
	0.1	9.4 ± 0.1	12.78 ± 0.07	16.7 ± 0.5	23.5 ± 0.4	0.54 ± 0.01
	0.2	9.4 ± 0.1	12.84 ± 0.08	16.9 ± 0.4	23.9 ± 0.4	0.54 ± 0.01
	0.3	9.45 ± 0.09	12.8 ± 0.1	17.1 ± 0.2	23.7 ± 0.4	0.55 ± 0.01

ϵ/k_BT, it is reversed for $\epsilon/k_BT \simeq 0.3$, which, as will be discussed, corresponds to values in the Θ region.

The change of dimensions with solvent conditions, with the other variables fixed, does not present any unexpected feature. For small and intermediate values of Φ, the latter well beyond the overlapping critical value, Φ*, the dimensions decrease for increasing polymer–polymer interactions. Only for our highest concentration, Φ = 0.75, is there not a definite variation trend (when one considers the higher uncertainties obtained in this case, due to difficulties in the thermal equilibration). Since this case is close to the melt, a significant influence of solving conditions cannot be intuitively predicted. For dilute systems and long chains, one can notice a dramatic decrease of dimensions for poorer solving conditions, as the chain collapses from the coil (good solvent) state to a globular conformation for sub-Θ temperatures.

For constant concentration and solving conditions, the variation with chain length can be studied by means of exponents ν_R and ν_S (which will be generically denoted as ν), calculated from fittings of the type

$$\langle R^2 \rangle^{1/2} \sim (N-1)^{\nu_R} \tag{6}$$

and

$$\langle S^2 \rangle^{1/2} \sim (N-1)^{\nu_S} \tag{7}$$

These exponents are contained in Tables I and II. For a single chain, the exponents vary from values very close to the theoretical critical exponent[3] of excluded-volume chains, $\nu = 0.588$, for $\epsilon/k_BT = 0$ to values close to the rigid sphere limit of $^1/_3$ for high polymer–polymer interactions (collapse state). The exponents are close to $^1/_2$ for $\epsilon/k_BT \simeq 0.3$, which is tentatively assigned as within the Θ region. However, comparison with previous results[7,16] indicates a noticeable variation of the exponents with the considered range of chain lengths in the vicinity of the Θ temperature. Thus, the calculations performed by McCrackin et al.[16] with long chains yielded $\epsilon/k_B\Theta = 0.275$ for the Θ temperature. In fact, our results for $\langle R^2 \rangle$ with $\epsilon/k_BT = 0.275$ have been fitted to the alternative nonlinear equation

$$\langle R^2 \rangle / b^2 = a(N-1)^{2\nu}[1 - c/\ln (N-1)] \tag{8}$$

which contains logarithm corrections[3] in the form predicted by the renormalization group theory.[17] We get $2\nu = 0.98$, $a = 2.17$, and $c = 0.73$, with a reduction of about 50% of the relative sum of squared deviations with respect to the fit to eq 6. An ideal nonreversal random walk would yield $\langle R^2 \rangle / b^2(N-1) = 1.5$, for a long chain in a simple cubic lattice.[4] The higher value obtained in our fitting for the equivalent parameter a should be attributed to ternary interactions. (An increase of $\langle R^2 \rangle$ in Θ conditions, with respect to the corresponding unperturbed chain average, is found in different simulations with attractive–repulsive potentials.[16,18])

The values of ν for good solvent conditions and higher polymer concentrations differ from the single-chain critical exponent approaching to $\nu = ^1/_2$ as Φ increases. However, this behavior is reversed for poorer solvent conditions. Thus, for $\epsilon/k_BT = 0.3$ we find that the mean dimensions and ν exhibit a slight increase from $\nu = ^1/_2$ for increasing concentrations. Therefore, it seems that, in the case of polymers close to the Θ region, an increase of concentration beyond Φ* causes a moderate expansion of the chains, as an efficient way to minimize the number of polymer–solvent contacts with additional intermolecular polymer–polymer interactions. It is not clear whether this effect is an artifact due to the lattice restrictions or constitutes a feature of real chains. Experimental work, for instance, neutron-scattering data, will be very useful to clarify this point.

(b) Scattering Form Factor. The form factor of a single chain has been evaluated from the formula

$$P(q) = (1/N^2)\sum_i^N \sum_j^N \langle \sin (qR_{ij})/qR_{ij} \rangle \tag{9}$$

with the same sampling techniques described above, and we have analyzed the dependence of P with $x = q^2\langle S^2 \rangle$, a variable that takes care of the influence of the global size of the chain. Once the results are scaled this way, we have found very small changes in the function $P(x)$ with the different variables (chain length, solvent conditions, or concentration). As an illustration, we have plotted in Figure 1 some of the curves, together with the results corresponding to the Debye formula (valid for long Gaussian chains)

$$P(x) = (2/x^2)(x - 1 + e^{-x}) \tag{10}$$

and those corresponding to a nonreversal random walk in the simple cubic lattice (unperturbed chain). It is observed that all our simulation results lie in a single curve, in spite of different values of N, ϵ/k_BT, and Φ, while the theoretical and ideal chain results are also very close to them, showing a marginal difference for the highest values of x.

(c) Sum of Reciprocal Averages and Diffusion Coefficient. We have calculated the sum of reciprocal

Table III
Results for D_0 from Equation 11

	$(D_0\xi/k_BT) \times 10^2$				
ϵ/k_BT	$N = 36$	$N = 48$	$N = 60$	$N = 84$	ν_D
0	11.12 ± 0.01	9.39 ± 0.01	8.25 ± 0.02	6.76 ± 0.02	0.575 ± 0.003
0.1	11.34 ± 0.01	9.62 ± 0.01	8.47 ± 0.02	6.96 ± 0.02	0.562 ± 0.003
0.2	11.63 ± 0.02	9.91 ± 0.01	8.76 ± 0.02	7.31 ± 0.02	0.534 ± 0.003
0.275	11.87 ± 0.02	10.20 ± 0.02	9.05 ± 0.02	7.60 ± 0.03	0.518 ± 0.004
0.3	11.97 ± 0.02	10.29 ± 0.02	9.14 ± 0.03	7.75 ± 0.03	0.508 ± 0.004
0.32	12.07 ± 0.02	10.37 ± 0.02	9.31 ± 0.03	7.88 ± 0.03	0.496 ± 0.004
0.34	12.15 ± 0.02	10.49 ± 0.02	9.43 ± 0.02	8.00 ± 0.03	0.485 ± 0.004
0.4	12.37 ± 0.02	10.81 ± 0.02	9.70 ± 0.03	8.48 ± 0.03	0.446 ± 0.004
0.5	12.91 ± 0.02	11.38 ± 0.02	10.41 ± 0.03	9.26 ± 0.03	0.394 ± 0.004

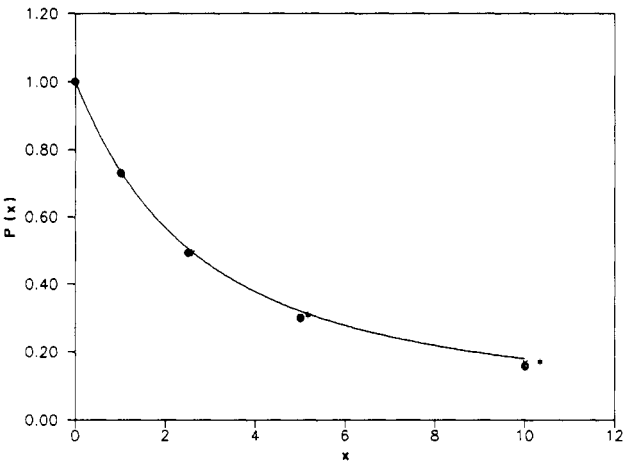

Figure 1. Individual form factor function $P(x)$ vs x for different solvent conditions, chain lengths, and concentrations. (×) N = 84, single chain, $\epsilon/k_BT = 0$. (+) $N = 36$, single chain, ϵ/k_BT = 0.3. (○) $N = 36$, $\Phi = 0.75$, $\epsilon/k_BT = 0$. The Debye formula curve (solid line) and the nonreversal random walk of $N = 84$ units (*) are also included.

distances between different units, also from the coordinates of the chains contained in different Monte Carlo cycles. The means are our estimations for S_r, defined in the Introduction. We omit here a report on these numerical values, since the results for nondilute systems do not have any clear direct application, and, at any rate, they correlate very clearly in their qualitative trends with the inverses of the corresponding mean dimensions. However, the results for single chains deserve a particular analysis, since they can be applied to the calculation of the translational diffusion coefficient according to the approximate Kirkwood formula

$$D_0 = (k_BT/\xi N)[1 + (1/N)\sigma S_r] \qquad (11)$$

where ξ is the friction coefficient of a chain unit and σ is its hydrodynamic radius (introduced as a parameter that gauges the hydrodynamic interactions[4]). For $\sigma = 0$, eq 11 leads to the simple result corresponding to the Rouse dynamics, $D_0 \sim N^{-1}$, which should coincide with the result obtained from the displacement of the center of masses (Einstein formula) in a Monte Carlo dynamic simulation. However, we adopt $\sigma/b = 0.256$, coherent with the value expected for a flexible statistical (Gaussian) subchain. In Table III, we show our values for D_0, calculated for different chain lengths and solvent conditions. It can be noticed that the variations with varying ϵ/k_BT are smaller than in the case of mean dimensions, though a sharp change for $\epsilon/k_BT > 0.3$ is also manifested for the longer chains, due to the coil to globule collapse. We have performed log–log linear regression analysis of D vs $1/(N-1)$. The fitted slopes (or exponents) ν_D are also shown in Table III. It can be observed that they are very similar to the exponents found for dimensions, though the values for the sub-Θ region are slightly higher.

Table IV
Results for $\rho = \langle S^2\rangle^{1/2}/R_h$

	ρ		
N	$\epsilon/k_BT = 0$	$\epsilon/k_BT = 0.275$	$\epsilon/k_BT = 0.5$
36	1.505 ± 0.006	1.426 ± 0.008	1.312 ± 0.007
48	1.518 ± 0.007	1.43 ± 0.01	1.301 ± 0.009
60	1.52 ± 0.01	1.44 ± 0.01	1.276 ± 0.011
84	1.53 ± 0.02	1.44 ± 0.02	1.212 ± 0.014

An interesting parameter, due to its weak dependence on the chain length, is the ratio of the mean radius of gyration of the chain to its hydrodynamic radius, $\rho = \langle S^2\rangle^{1/2}/R_h$, where R_h can be obtained from the Stokes–Einstein relationship $k_BT/D_0 = 6\pi\eta_0 R_h$. η_0 is the solvent viscosity, which can be eliminated through the Stokes equation for the friction coefficient of a single unit, $\xi = 6\pi\eta_0\sigma$. Then, in practical units

$$\rho = (D_0\xi/k_BT)(\langle S^2\rangle^{1/2}/\sigma) \qquad (12)$$

Our results for ρ are shown in Table IV. It can be observed that ρ decreases for poorer solvent conditions. The dependence on N is small, but its trend changes with ϵ/k_BT. Regression analysis of the type ρ vs $(N-1)^{-1/2}$ has been performed in order to estimate the extrapolated long-chain limiting values. Thus, we get $\rho = 1.58 \pm 0.04$ for $\epsilon/k_BT \simeq 0$ (good solvents), in good agreement with the result $\rho = 1.59 \pm 0.03$, which we have recently obtained[19] also by extrapolation of values obtained through eqs 11 and 12 with S_r and $\langle S^2\rangle$ calculated from off-lattice Brownian dynamics trajectories of chains with Gaussian units and a repulsive potential.[20] The extrapolated value for $\epsilon/k_BT = 0.275$ (Θ region) is $\rho = 1.48 \pm 0.04$, also in agreement with the result $\rho = 1.508$ obtained from eq 11 and an exact evaluation of D_0 for a long Gaussian chain.[4] Then, it seems that the lattice restrictions are not introducing any distortion in these limits, which, therefore, can be considered as model independent. A decrease of ρ due to excluded-volume effects with respect to its Θ region value is predicted by the renormalization group theory,[21] as a consequence of the higher permeability of expanded chains, and it is also in agreement with most experimental data.

The results for ρ in the sub-Θ region ($\epsilon/k_BT = 0.5$) exhibit a lower correlation in the regression analysis. The extrapolated value obtained by ignoring the smallest chain is $\rho = 0.95 \pm 0.06$, which is closer to the value corresponding to a rigid sphere, $\rho = 0.77$, than to the coil limits in good or Θ solvents. Then, the collapse of the chains to adopt a globular structure is clearly manifested.

It should be mentioned that the values of ρ calculated from the Kirkwood formula constitute an upper value of the actual values,[22,23] which can only be obtained through dynamic simulations with fluctuating hydrodynamic in-

Table V
Results for $F(R\to0)$ and α

Φ	ϵ/k_BT	$F(R\to0)\times10^4$ $N=36$	$N=48$	$N=60$	$N=84$	α
single chain	0	3.3 ± 0.1	1.79 ± 0.09	1.23 ± 0.07	0.62 ± 0.06	1.93 ± 0.09
	0.3	6.9 ± 0.2	4.7 ± 0.2	3.2 ± 0.2	2.4 ± 0.1	1.25 ± 0.06
0.38	0	4.9 ± 0.1	3.0 ± 0.1	2.47 ± 0.08	1.39 ± 0.06	1.42 ± 0.05
	0.3	6.4 ± 0.1	4.0 ± 0.1	3.0 ± 0.1	1.77 ± 0.07	1.49 ± 0.04

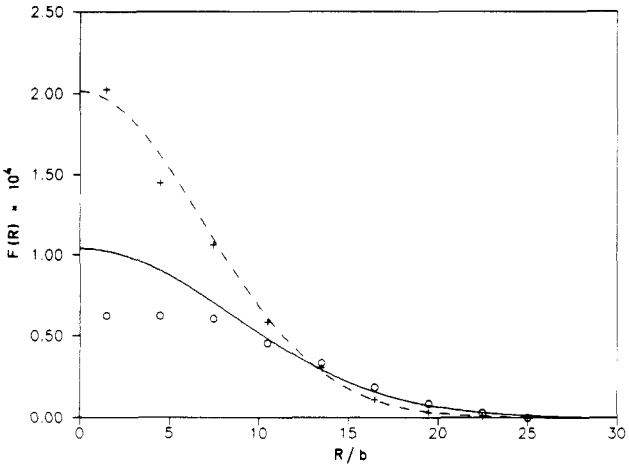

Figure 2. $F(R)$ vs R (in reduced units) for a single chain of 84 units with $\epsilon/k_BT = 0$ (O) and $\epsilon/k_BT = 0.275$ (+). The solid and dashed lines represent results from the Gaussian function (eq 13) corresponding to the averages $\langle R^2\rangle$ obtained for each case.

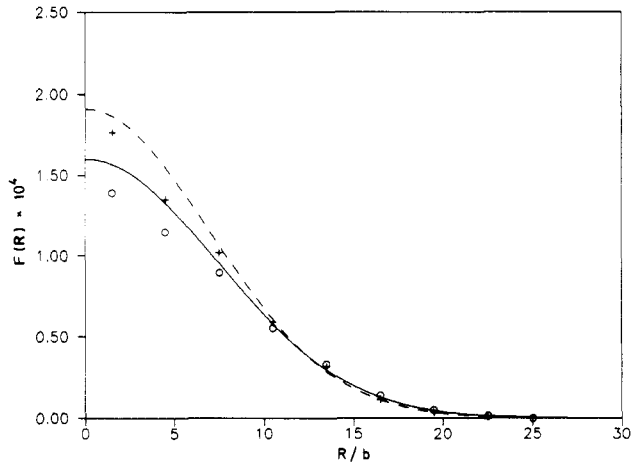

Figure 3. As in Figure 2, but with results for a chain with 84 units, with $\Phi = 0.38$ and ϵ/k_BT (O) or 0.3 (+).

teractions. Previous investigations for off-lattice models[19,23] indicate that the rigorous results may differ 10–15% for Θ and good solvent conditions.

(d) Distribution Function. The distribution function of the end-to-end distance provides an incisive description of a flexible chain, determining many of its conformational properties. This function can be easily evaluated in simulation conformational samplings by means of the computation of histograms that correspond to adequate grids of values of R. The histogram results are then normalized according to the total number of simulation cycles involved in their calculation (similar to the number employed in the calculation of averages) and also to the volume associated with the given grid interval, in order to obtain the probability density, $F(R)$. (If one is interested in the calculation of the radial distribution function, $4\pi R^2F(R)$, this volume should be substituted by the grid interval length.)

We show in Figures 2 and 3 the results obtained for our longest chain. In Figure 2, we plot the single-chain functions for good Θ solvents. It is apparent that solvent conditions have a fundamental influence on the curve shapes. The Θ curve is very close to the theoretical Gaussian function

$$F(R) = (3/2\pi\langle R^2\rangle)^{3/2}\exp(-3R^2/\langle R^2\rangle) \qquad (13)$$

where, as previously explained, we have adopted for $\langle R^2\rangle$ the Θ region average calculated with $\epsilon/k_BT = 0.275$. However, the good solvent distribution function is no longer described by Gaussian functions defined from $\langle R^2\rangle$, and one can observe a depression of $F(R)$ for the smallest values of R. This depression has been theoretically described as a correlation hole effect.[3] The effect has also been reproduced in off-lattice simulations[20] (where, in fact, an even more remarkable depression is found, due probably to the absence of lattice restrictions).

The results for more concentrated systems are shown in Figure 3. We can notice that the depression for small R is greatly diminished, and both the good solvent and Θ region curves are fairly well described by Gaussian functions.

The influence of the correlation function on properties of interest is apparent since the distribution function in the proximity of $R = 0$ is directly related to calculations for equilibrium cyclization constants, according to procedures inspired in the Jacobson–Stockmayer theory.[24] The dependence on N of our results for the grid with the smallest value of R, $F(R\to0) \simeq F(0)$, has been analyzed by means of linear log–log fits to scaling laws of the type

$$F(R\to0) \sim (N-1)^{-\alpha} \qquad (14)$$

The results are contained in Table V. The good solvent value of α for a single chain is in excellent agreement with the correlation hole theory[3,24] (in spite of its high error interval). For the Θ solvent and more concentrated systems, the results are smaller than (though generally close to) the value $\alpha = 1.5$, expected for a chain that obeys the Gaussian distribution for R. The differences and higher uncertainties should be attributed to lattice effects and numerical problems associated with the grid procedure.

In any case, we can conclude that the cyclization constants of dilute chains and their dependence on chain length or molecular weight are significantly affected by both solvent conditions and concentration, through the influence of these variables on the end-to-end distance distribution function.

Acknowledgment. This work has been supported in part by Grant PB89-0093 of the DGICYT. A.L.R. acknowledges a Fellowship from the PFPI.

References and Notes

(1) Binder, K. In *Molecular Level Calculations of the Structures and Properties of Non-Crystalline Polymers*; Bicerano, J., Ed.; Marcel Dekker: New York, 1989.
(2) López Rodriguez, A.; Wittmann, H.-P.; Binder, K. *Macromolecules* **1990**, *23*, 4327.

(3) de Gennes, P.-G. *Scaling Concepts in Polymer Physics*; Cornell University: Ithaca, NY, 1979.
(4) Yamakawa, H. *Modern Theory of Polymer Solutions*; Harper and Row: New York, 1971.
(5) Madras, N.; Sokal, A. D. *J. Statis. Phys.* **1988**, *50*, 109.
(6) Verdier, P. H.; Stockmayer, W. H. *J. Chem. Phys.* **1962**, *36*, 227.
(7) Gurler, M. T.; Crabb, C. C.; Dahlin, D. M.; Kovac, J. *Macromolecules* **1983**, *16*, 398.
(8) Kolinski, A.; Skolnick, J.; Yaris, R. *J. Chem. Phys.* **1986**, *85*, 3585.
(9) Kolinski, A.; Skolnick, J.; Yaris, R. *J. Chem. Phys.* **1986**, *84*, 1922.
(10) Kremer, K. *Macromolecules* **1983**, *16*, 1632.
(11) Bishop, M.; Frinks, S. *J. Chem. Phys.* **1987**, *87*, 3675.
(12) Okamoto, H. *J. Chem. Phys.* **1983**, *79*, 3976.
(13) Richards, R. W.; Maconnachie, A.; Allen, G. *Polymer* **1978**, *19*, 266.
(14) Crabb, C. C.; Kovac, J. *Macromolecules* **1985**, *18*, 1430.
(15) Kolinski, A.; Skolnick, J.; Yaris, R. *J. Chem. Phys.* **1987**, *86*, 7164.
(16) McCrackin, F. L.; Mazur, J.; Guttman, L. M. *Macromolecules* **1973**, *6*, 859.
(17) Freed, K. F. *Renormalization Group Theory of Macromolecules*; Wiley: New York, 1987.
(18) Freire, J. J.; Pla, J.; Rey, A.; Prats, R. *Macromolecules* **1986**, *19*, 452.
(19) Rey, A.; Freire, J. J.; Garcia de la Torre, J. *Macromolecules*, in press.
(20) Rey, A.; Freire, J. J.; Garcia de la Torre, J., submitted for publication in *Polymer*.
(21) Wang, S.-Q.; Douglas, J. F.; Freed, K. F. *Macromolecules* **1985**, *18*, 2464.
(22) Rotne, J.; Prager, S. *J. Chem. Phys.* **1969**, *50*, 4831.
(23) Fixman, M. *J. Chem. Phys.* **1983**, *78*, 1588; **1983**, *78*, 1594.
(24) Semlyen, J. A. In *Cyclic Polymers*; Semlyen, J. A., Ed.; Elsevier: London, 1986.